

EFFECTS OF SEBS AND SEBS-g-MA MODIFICATIONS ON THE FRACTURE BEHAVIOR OF i-PP/GLASS BEAD AND i-PP/WOLLASTONITE COMPOSITES

**Onur BALKAN^a, Halil DEMİRER^b, Ayhan EZDEŞİR^c, Hüseyin YILDIRIM^d
and Ülkü YILMAZER^e**

^a Marmara University, Institute for Graduate Studies in Pure and Applied Science, Metal Education, Göztepe Campus, 34722 Kadıköy, İSTANBUL

^b Marmara University, Technical Education Faculty, Metal Education, Göztepe Campus, 34722 Kadıköy, İSTANBUL

^c Petkim Petrokimya Holding A.Ş., Research-Development Center, 35801, Aliağa, İZMİR

^d Yıldız Technical University, Faculty of Arts and Science, Department of Chemistry, Davutpaşa Campus, 34220, Esenler, İSTANBUL

^e METU, Faculty of Engineering, Department of Chemical Engineering, 06531, ANKARA

ABSTRACT

The effects of elastomer types and volume fractions on the fracture behavior of polypropylene composites were investigated. Isotactic-polypropylene (i-PP) was used as matrix, polystyrene-*b*-poly(ethylene-co-butylene)-*b*-styrene (SEBS) and the corresponding block copolymer grafted with maleic anhydride (SEBS-g-MA) were used as thermoplastic elastomers. Spherical shaped glass bead and acicular shaped wollastonite were used as fillers. Firstly, polypropylene/filler composites were compounded with 20 volume percent filler; secondly, the composites were modified with SEBS and SEBS-g-MA at 2.5, 5 and 10 % by volume. Fracture behavior of composites was evaluated by Izod Impact tests and results were supported by SEM micrographs. Interfacial interactions between inorganic particulates and SEBS-g-MA elastomer phases were revealed by FT-IR. It was found that fracture behavior of composites strongly depend on geometrical shapes of inorganic fillers, volume fractions of components, interfacial interactions between phases and phase morphology. SEM investigations indicated that (PP/filler)/SEBS composites exhibit separation of the filler and the elastomer phases in PP matrix. However, (PP/filler)/SEBS-g-MA composites exhibited encapsulation of the filler by the elastomer phase (core-shell morphology). The resultant morphology gave rise to improved toughness. It was found that (PP/wollastonite)/SEBS-g-MA composites have superior impact strength due to the enhanced adhesion at the interfaces of composites and reinforcing effect of wollastonite particles.

Keywords: Core-shell, elastomer, glass bead, polypropylene, wollastonite.

1. INTRODUCTION

Thermoplastics, such as polypropylene (PP), are widely used in many scientific, industrial and daily applications since they are versatile and low cost materials. In addition, their mechanical properties can be improved by incorporation of fillers and elastomers. In this case, the incorporation of rigid fillers and/or elastomers into polypropylene matrix affects the properties of resultant composites in different ways. It is well known that, composites have a higher performance range than their individual components. However, addition of rigid fillers enhances stiffness of the composite at the expense of toughness. The opposite was found approximately for addition of elastomer which often increases toughness but reduces the stiffness of composites. It can be said that careful incorporation of both filler and elastomer in a composite could result in an optimum mechanical performance. A stiffness-to-toughness balance which depends on filler and elastomer ratios is shown schematically in Fig. 1. The stiffness-to-toughness balance route was extensively studied in various composites [1-3].

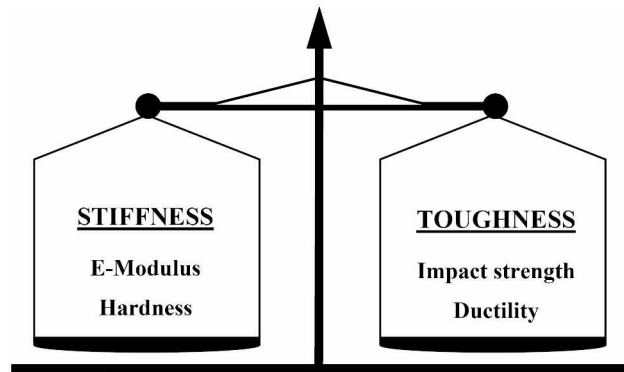


Fig. 1. A schematic of stiffness-to-toughness balance and optimisation in composites.

With the developments in materials science, creation of a composite both stiffer and tougher than the matrix material with low cost has become important. In 1967, Matonis and Small [4,5] proposed that encapsulation of rigid spherical inclusions within a thin layer of low-modulus elastomer could result in hybrid composites exhibiting improved toughness without sacrificing stiffness with respect to polypropylene matrix (Fig. 2). This structure is called “core-shell morphology”. They also proposed that the most sensitive variable is the thickness of elastomer layer, and only very thin elastomer layers were admissible (Eq. 1).

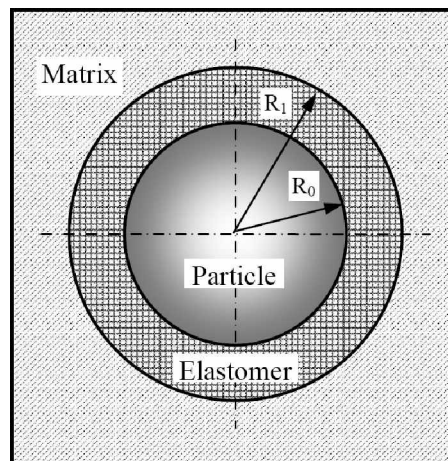


Fig. 2. Core-shell morphology in polymer composites [4,5].

$$\frac{R_0}{R_1} \cong 0,999 \quad (1)$$

where R_0 and R_1 are radiuses of a spherical particle of filler and elastomer layer, respectively. Several papers have been concerned on the core-shell composites, such as PP/glass bead/SEBS-g-MA [6-9], PP/EPR-g-MA/glass bead [10], PP/EPDM/glass bead [11], PP/SEBS-g-MA/talc [12,13], PP/talc/SEBS-g-MA [14], PP/EPR-g-MA/CaCO₃ [15,16], PP/SEBS-g-MA/short glass fiber [17-20], PP/sisal fiber/SEBS-g-MA [21], PP/vermiculite/SEBS-g-MA [22]. The aim of this work is to create core/shell morphology in the composites and investigate effects of core-shell morphology on fracture behavior of polypropylene/glass bead and polypropylene/wollastonite composites.

2. EXPERIMENTAL

2.1 Materials

Isotactic polypropylene used as the matrix material in this work is Petoplen MH418, supplied by Petkim. It has a melt flow rate of 4-6 g 10min⁻¹ and a density of 0.886 g cm⁻³. Glass bead and wollastonite were selected as the filler. Glass bead is Spheriglass[®] Grade 3000 CP03/CP01, supplied by Potters Industries Inc. It was solid spherical particles with a mean diameter of 12-26 μm, a density of 2.5 g cm⁻³. Wollastonite (CaSiO₃) is Nyglos[®] 8, supplied by Nyco Minerals, Inc. It was acicular particles with a L/D of 19/1 (150 μm/8 μm), a density of 2.9 g cm⁻³. In order to clean the surfaces, filler particles were heated in an oven at 600 °C for 6 h before compounding.

2.2 Preparation of Samples

Compounding is an effective way of developing new materials to achieve optimum balance between performance and cost. Two-phase composites with varying contents from 10 to 30 vol. % of filler were compounded in an intermeshing co-rotating twin-screw extruder (Thermo Prism, Haake, a screw diameter of 16mm, a L/D ratio of 25) at a screw speed of 100 r.p.m. The barrel temperature profile was set between 150 °C and 230 °C (from feed zone to die). Then, three-phase composites were compounded. 2.5, 5 and 10 vol. % of SEBS or SEBS-g-MA were incorporated into the two-phase (dual) composites which consisted of 20 vol. % of filler. The resulted composites were pelleted and, then, were molded as rectangular strips using an injection molding machine with the barrel temperature profile was set at 230 °C and a mold temperature of 40 °C.

2.3 Testing

Izod impact tests were performed according to TS 1005 [23] using a Zwick model impact testing machine with a pendulum of 5.4 J on notched rectangular strips of 12.5 × 3.2 × 62 mm³ at room temperature as shown in Fig. 3. Electron micrographs of gold-coated fracture surfaces of the specimens were taken with a JEOL JSM-5910LV scanning electron microscope at 10 kV. The samples, which were fractured at liquid nitrogen temperature, were analyzed with SEM. Fourier transform infrared (FT-IR) spectra were obtained using a Thermo Nicolet, spectrometer, Nexus 670 FT-IR E.S.P.[™]. In order to obtain the spectra of the composites, thin films with a thickness of 150 ± 5 μm and a diameter of 15 mm were prepared in a hot press. Spectra were made up of 64 scans with a resolution of 4 cm⁻¹.

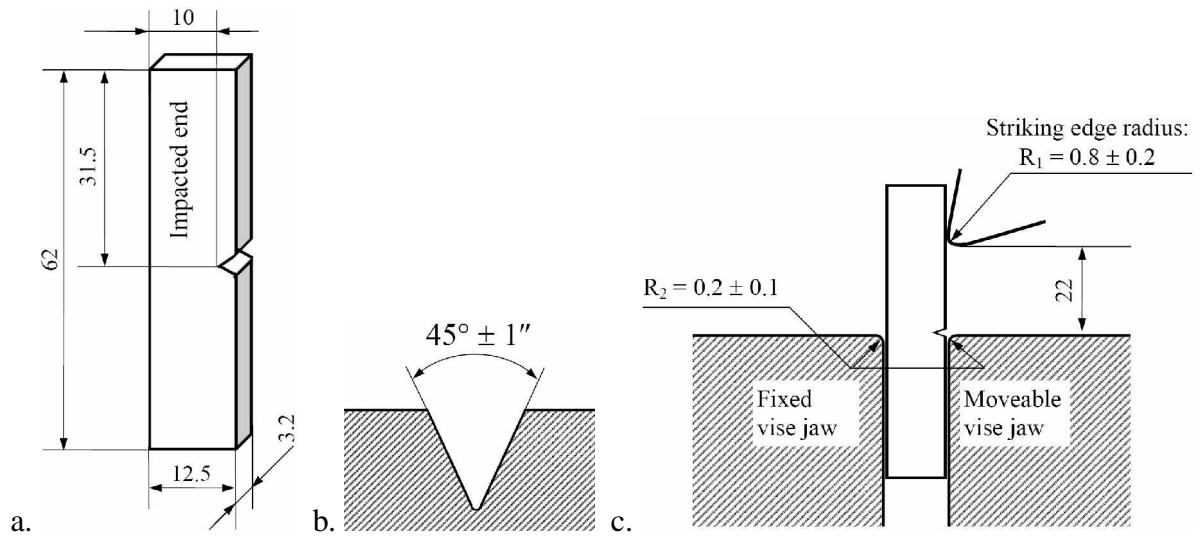


Fig. 3. (a) Dimensions of an Izod type test specimen. (b) The notch (type A). (c) Relationship of vise, specimen and striking edge to each other [23].

3. RESULTS AND DISCUSSIONS

3.1 Dual Composites

Impact strength vs. filler content of two-phase composites, PP/glass bead and PP/wollastonite composites, are plotted in Fig. 4. Impact strength of PP/glass bead composites increased slightly up to 10 vol. % of glass bead, and then, decreased with increasing glass bead ratios. It was reported that the fracture energy of a composite could be increased by a rigid particulate-filler. However, the degree of toughness enhancement depends upon both the volume fraction and particle size of the filler. It was proposed that the process largely responsible for this increased toughness is “the crack-pinning mechanism” as shown schematically in Fig. 5 [24].

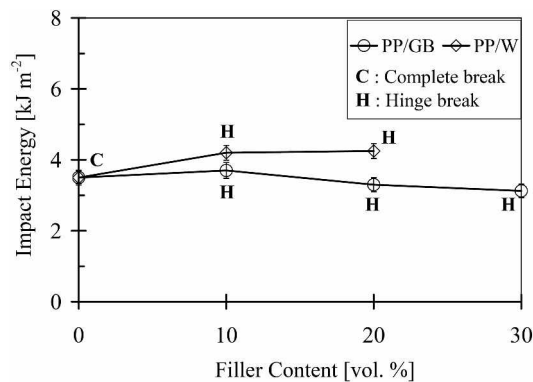


Fig. 4. Impact strengths of PP/glass bead (PP/GB) and PP/wollastonite (PP/W) composites as a function of filler volume fraction.

According to the crack-pinning mechanism, the toughening may occur by the interactions of the moving crack front with dispersed rigid particulate-filler i.e. obstacle pinning of the crack causing the crack front to bow out between the rigid particulate-filler. During the initial stage of crack propagation both a new fracture surface is formed and the length of the crack front is increased due to its change of shape between the pinning positions. The fractional increase in crack-front length per unit crack extension will depend upon the particle spacing. The energy is not only required to create new fracture surface but it must also be supplied to the newly formed length of crack front which is assumed to possess a line energy [24].

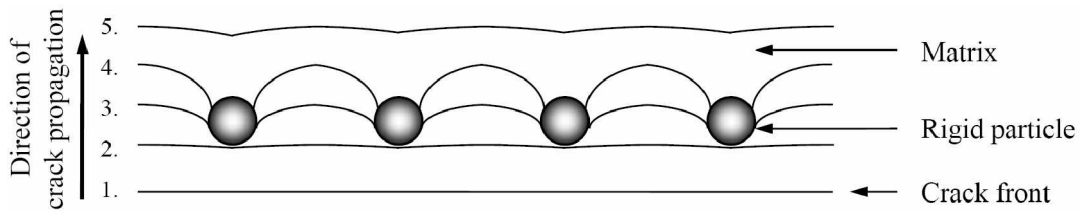


Fig. 5. Stages of the crack-pinning mechanism in a rigid particulate-filled composite (schematic presentation) [24]

PP/wollastonite composites absorbed higher impact energy than PP/glass bead composites as shown in Fig. 4. It can be explained that reinforcement effect of acicular wollastonite particles increase strength of composites. The microscopic failure mechanisms occurring in discontinuous fiber-reinforced thermoplastics are shown schematically in Fig. 6. They can be classified into matrix-related (crazing, voiding, fracture and shear yielding) and fiber-related (debonding, pull-out and fracture) mechanisms. It was mentioned that the relative orientation of the fibers with respect to the crack growth strongly affects the onset and type of the above absorption mechanism [25].

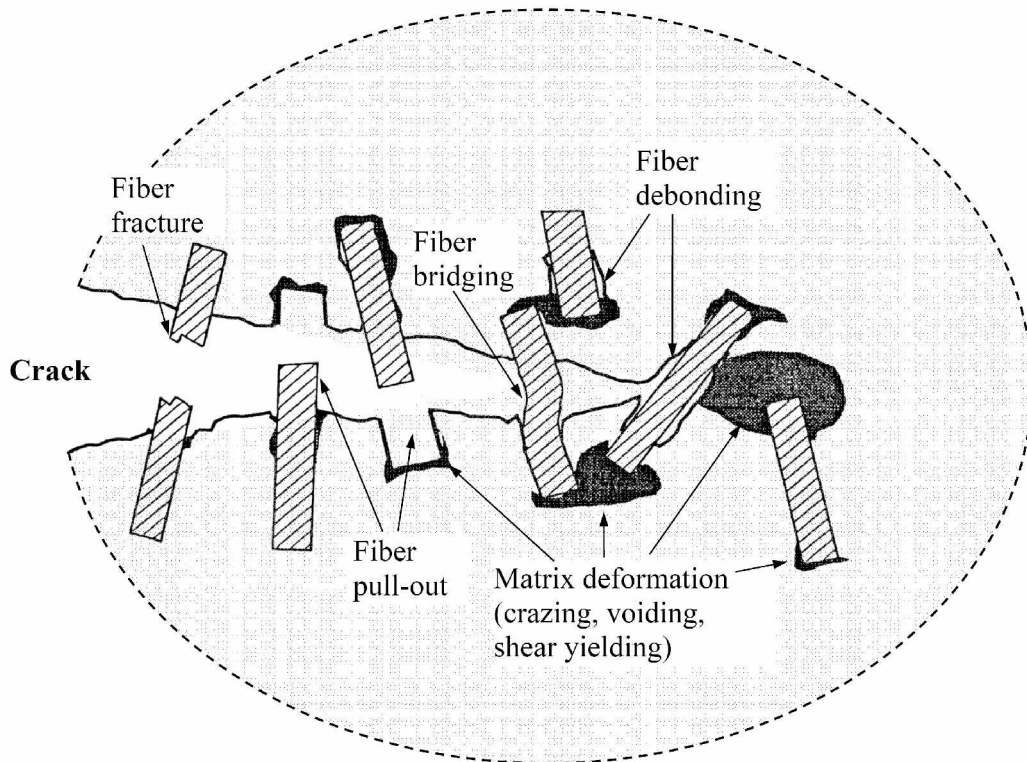


Fig. 6. Failure mechanisms of discontinuous fiber-reinforced thermoplastics (schematic) [25]

In addition, neat polypropylene samples were broken completely while all two-phase composites exhibited hinge break behavior as shown in Fig. 4. Hinge break type of failure is described as an incomplete break in which one part of the specimen cannot support itself above the horizontal when the other part is held vertically (less than 90° included angle) [23]. It can be explained by “the skin-core structure” of composites since the core of the specimens has higher filler ratios than outer region (skin). During the cooling of a polymer composite in an injection mould, particles of fillers may be driven into the core of the part [26].

3.2 Ternary Composites

SEM micrographs of ternary composites are shown in Fig. 7. SEM investigations on fractured surfaces of samples revealed that two kinds of phase structure formed depending on the elastomer type. These are either a separate dispersion of the elastomer phase or encapsulation of the filler particles by elastomer. The ternary composites that have SEBS elastomer exhibited separately dispersed phase morphology. The interfacial bonding between the particle of filler and polymer was relatively poor in the composites containing SEBS, as observed by clean particle surfaces shown in Figs. 7 (a) and (c) and, the pull-out behavior observed in Fig. 7 (c). Modifications of the polypropylene composites with SEBS-g-MA have resulted in elastomer encapsulation of filler particles as shown in Figs. 7 (b) and (d), called core-shell morphology.

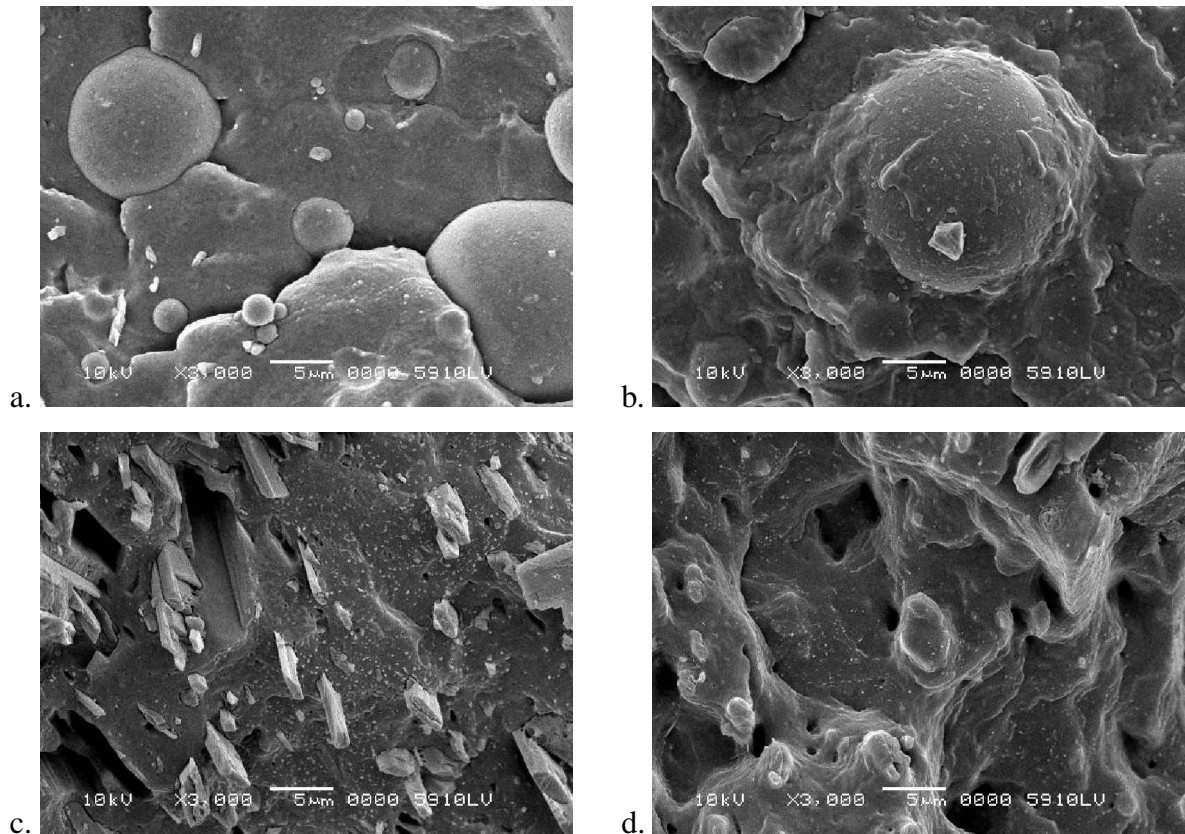


Fig. 7. SEM micrographs of ternary composites. (a) (PP/glass bead)/SEBS, (b) (PP/glass bead)/SEBS-g-MA, (c) (PP/wollastonite)/SEBS, and (d) (PP/wollastonite)/SEBS-g-MA composites with vol. ratio of (80/20)/10.

This was also confirmed by FT-IR absorption spectra for (PP/glass bead)/SEBS-g-MA and (PP/wollastonite)/SEBS-g-MA composites as shown in Figs. 8 (a) and (b), respectively. Maleic anhydride (MA) groups on SEBS-g-MA elastomer have two C=O bands due to the vibrational coupling of these groups [27-30]. These strong absorption bands are located at 1721 cm^{-1} (asymmetric stretching) and 1711 cm^{-1} (symmetric stretching) as shown in Fig. 9. The (PP/glass bead)/SEBS-g-MA and (b) (PP/wollastonite)/SEBS-g-MA composites showed new bands at 1736 cm^{-1} and 1711 cm^{-1} , respectively. The new bands have been assigned to interfacial interaction between elastomer and filler surface depicted in Fig. 9 which is believed to have formed due to an esterification reaction between MA group of SEBS-g-MA elastomer and surface of the fillers during extrusion and injection processing [31,32].

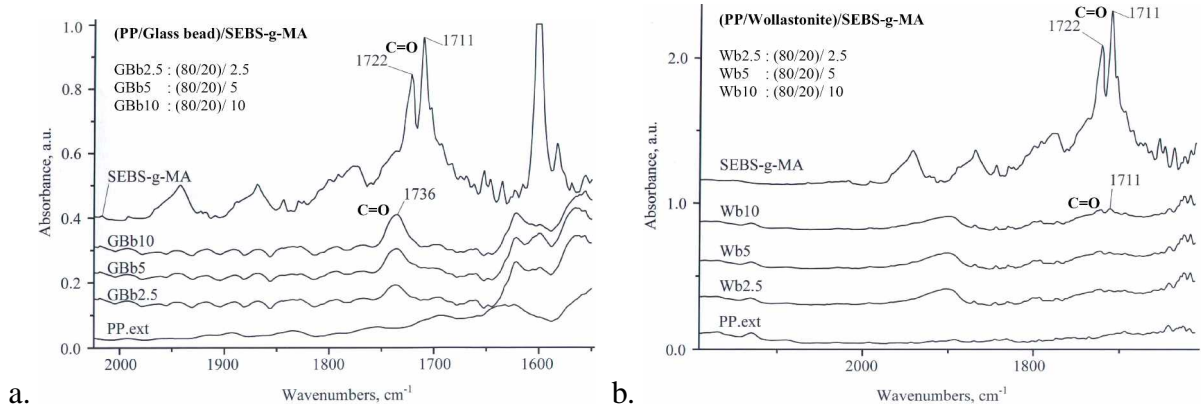


Fig. 8. FT-IR spectra of (a) (PP/glass bead)/SEBS-g-MA and (b) (PP/wollastonite)/SEBS-g-MA composites.

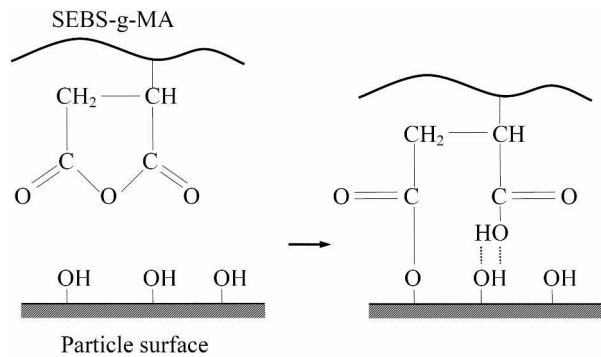


Fig. 9. An interfacial interaction between SEBS-g-MA and inorganic particle [31,32].

Impact strength of the composites increased with increasing elastomer content as shown in Figs. 10 (a) and (b). It was clearly shown that incorporation of SEBS-g-MA elastomer in the composites has a significant influence on impact strength of resultant composites. The increase in the impact strength of the composites with increasing SEBS-g-MA elastomer content is higher than those of SEBS elastomer due to the formation of core-shell morphology. Reinforcement effect of acicular particles of wollastonite further improved impact strength of ternary composites as shown in Fig. 10. The remarkable enhancement in the impact strength of (PP/wollastonite)/SEBS-g-MA composites indicated the effect of core-shell morphology and reinforcement effect of acicular wollastonite particles.

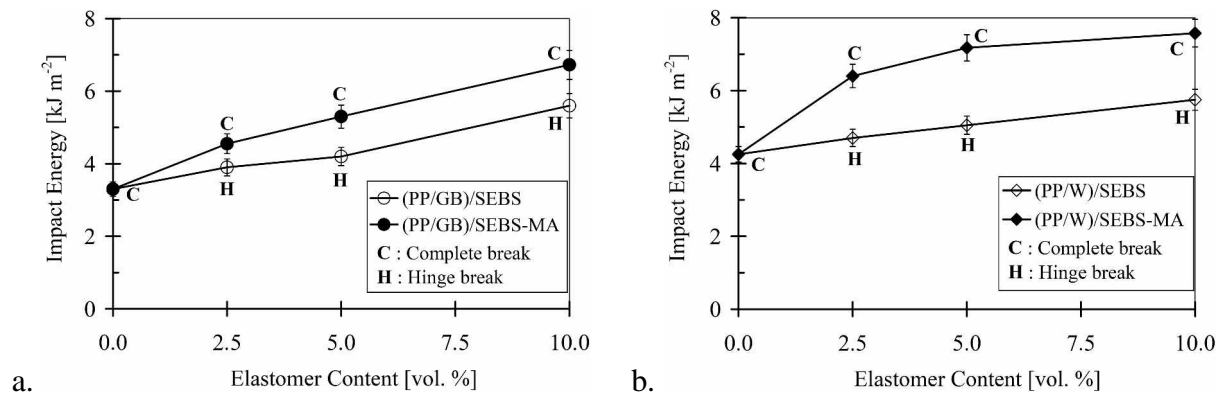


Fig. 10. Plots of impact strength vs. filler content of (a) (PP/glass bead)/elastomer and (b) (PP/wollastonite)/elastomer composites.

On the other hand, rigid filler particles forming cores in the core-shell composites apparently extend the elastomer volume fraction instead of stiffening the matrix, so that the rigidity of the composites may even decrease with increasing filler volume fraction. If the elastomer layer thickness in the core-shell composites is higher than that of Eq. 1, effective elastomer volume fraction ($\phi_{\text{eff.e}}$) can be calculated as Eq. 2 [13,16].

$$\phi_{\text{eff.e}} \cong \phi_e + \phi_f \quad (2)$$

where ϕ_e and ϕ_f are the elastomer and filler volume fractions in a core-shell ternary composites, respectively. This was explained by Matonis and Small [4,5] indicating that the effect of filler particles on the stiffness of composites depends primarily on elastic properties of the outer layer.

Fracture behaviors of the ternary composites containing glass bead and wollastonite are schematically presented in Fig. 11 and Fig. 12, respectively. When the elastomer and rigid filler particles are separated in the PP matrix as shown in Figs. 11(a) and 12(a), the filler particles may tend to produce a range of micro-cracks as impact is applied. Although elastomer particles can stop crack propagation, they would not be fully effective. Dominant failure mechanisms are debonding in the glass bead composites and pull-out in the wollastonite composites. It should be noted that fiber pull-out is the main energy dissipation mechanism during impact fracture for short fiber reinforced composites [25].

If the rigid filler particles were encapsulated by elastomer and formed a core-shell structure as shown in Figs. 11(b) and 12(b), the original micro-cracks initiate at the filler particles and crack propagation is prevented and yield zone around the elastomer particle is formed. In this case, elastomer phase can be fully effective on increasing the impact strength.

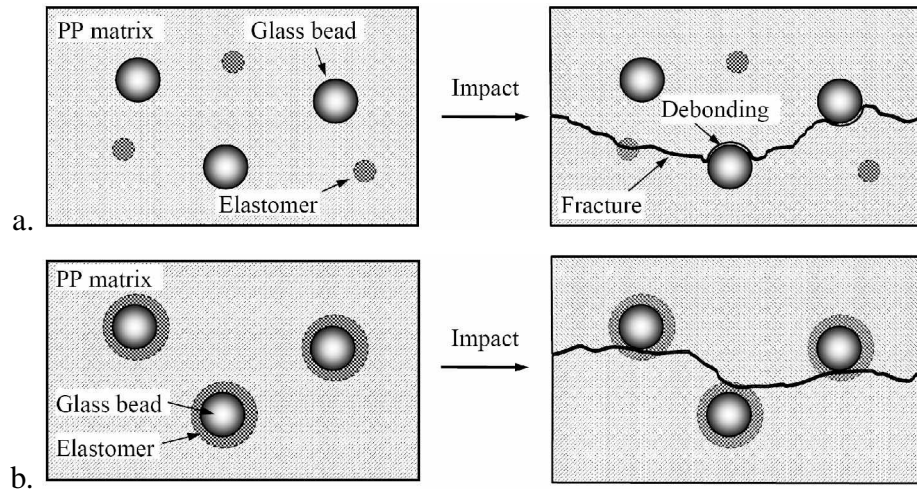


Fig. 11. Schematic representations of (a) (PP/glass bead)/SEBS and (b) (PP/glass bead)/SEBS-g-MA composites, which have separate-phase and core-shell morphologies, respectively.

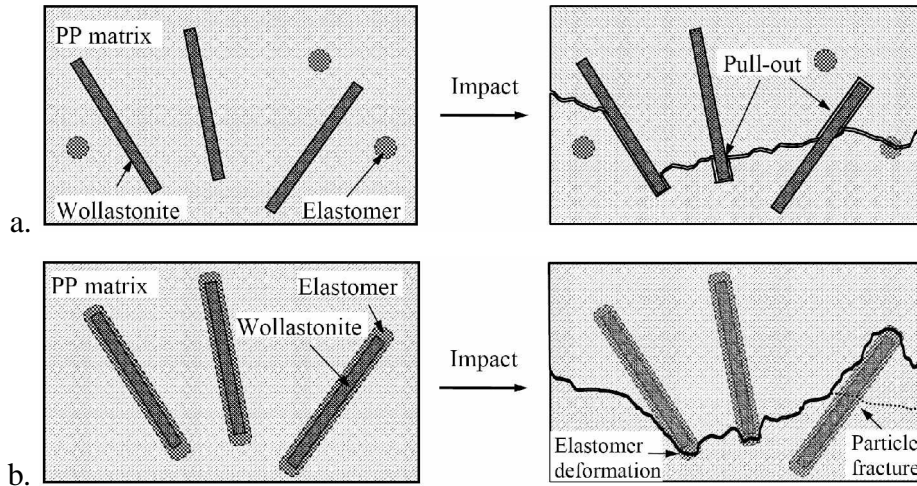


Fig. 12. Schematic representations of (a) (PP/wollastonite)/SEBS and (b) (PP/wollastonite)/SEBS-g-MA composites, which have separate-phase and core-shell morphologies, respectively.

Elastomer type also changed the fracture behavior of the composites. While dual-phase composites and ternary-composites containing SEBS elastomer exhibited a hinge break type of fracture, the composites including SEBS-g-MA fractured completely as shown in Fig. 10. In general, the hinge break type of fracture occurs in the composites which have skin-core micro-structure. Therefore, it should be noted that introduction of SEBS-g-MA elastomer into the composites promoted compatibility between filler and matrix, and diminished skin-core effect on the composites as shown schematically in Fig. 13. Wong and Mai [17] reported that incorporation of SEBS-g-MA into PP/PP6/short glass fiber composites reduced skin-core effect on the resultant composites.

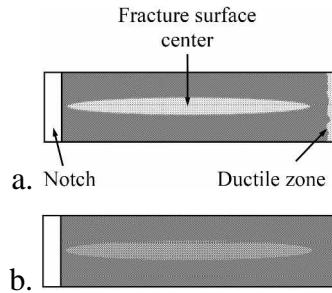


Fig. 13. Schematically presentations of fractured surfaces of composites. (a) Dual and ternary composites containing SEBS elastomer. (b) Ternary composites including SEBS-g-MA.

4. CONCLUSIONS

PP/wollastonite composites exhibited higher impact strength than PP/glass bead composites due to the reinforcement effect of acicular wollastonite particles.

Mechanical properties of ternary-composites were balanced by physically mixing the elastomers, rigid fillers and polypropylene matrix. Moreover, elastomer type in both composites has a very significant influence on the impact strength. The core-shell and separately dispersed phase morphologies were detected in the composites containing SEBS-g-MA and SEBS elastomer, respectively. SEBS-g-MA elastomer behaved as both compatibilizer and adhesion promoter in composites and increased impact strength. SEBS-g-

MA containing composites fractured completely whereas SEBS containing composites exhibited hinge break type of fracture. This shows the effect of SEBS-g-MA on the prevention of skin-core structure. It was found that (PP/wollastonite)/SEBS-g-MA composites have superior mechanical performance due to the higher adhesion at the interfaces of composites and reinforcing effects of wollastonite particles.

ACKNOWLEDGEMENTS

The authors would like to express their gratitude to Güralp Özkoç, Özcan Köysüren, Sertan Yeşil and Mert Kılınç, all of whom from METU, Department of Chemical Engineering, for their helps during the extrusion process. Thanks also go to M.Sci.Eng. Mustafa İlhan, Marmara University, Engineering Faculty, for SEM analysis.

REFERENCES

1. Comitov, P.G., Nicolova, Z.G., Simeonov, K., Naidenour, K.V. and Siarova, A.D., *European Polymer Journal*, 20(4) 405-407, 1984.
2. Pukanszky, B., Kolarik, J. and Lednický, F., "Polymer Composites", Ed. By Sedlacek, B., W. de Gruyter & Co., Berlin, 1986
3. Pukanszky, B., Tudos, F. and Kelen, T., *Polym. Compos.*, 7(2) 106-115, 1986
4. Matonis, V.A.: "An Analytical Evaluation of a Hypothetical Three-Phase Material", Ph.D. Thesis, The University of Connecticut, USA, 1967.
5. Matonis, V.A.; Small, N.C.: "A Macroscopic Analysis of Composites Containing Layered Spherical Inclusions", *Polym. Eng. Sci.*, 9(2) 90-99, 1969.
6. Stricker, F. and Mülhaupt, R., *J. Appl. Polym. Sci.*, 62(11) 1799-1806, 1996.
7. Stricker, F., Friedrich, C. and Mülhaupt, R., *J. Appl. Polym. Sci.*, 69(12) 2499-2506, 1998.
8. Stricker, F. and Mülhaupt, R., *Polymer Engineering and Sci.*, 38 (9) 1463-1470, 1998.
9. Mouzakis, D.E., Stricker, F., Mülhaupt, R. and Karger-Kocsis, J., *J. Mater. Sci.*, 33(10) 2551-2562, 1998.
10. Hornsby, P.R. and Premphet, K., *J. Mater. Sci.*, 32(18) 4767-4775, 1997.
11. Liang, J.Z., Li, R.K.Y. and Tjong, S.C. *Polym. Eng. Sci.*, 40 (9) 2105-2111, 2000.
12. Long, Y. and Shanks, R.A., *J. Appl. Polym. Sci.*, 62(4) 639-646, 1996.
13. Shanks, R.A. and Long, Y., *Polym. Networks Blends*, 7(2) 87-92, 1997.
14. Denac, M. and Musil, V. *Acta Chim Slov.*, 46(1) 55-67, 1999.
15. Kolarik, J., Lednický, F., Jancar, J. and Pukanszky, B., *Polymer Commun.*, 31 201-204, 1990.
16. Kolarik, J. and Jancar, J., *Polymer*, 33(23) 4961-4967, 1992.
17. Wong, S.-C. and Mai Y.-W., *Polym. Eng. Sci.*, 39(2) 356-364, 1999.
18. Tjong, S.C., Xu, S.-A., Li, R.K.Y. and Mai, Y.W., *Polym. Int.*, 51(11) 1248-1255, 2002.
19. Tjong, S.C., Xu, S.A. and Mai, Y.-W., *J. Polym. Sci.*, B40(17) 1881-1892, 2002.
20. Tjong, S.C., Xu, S.A. and Mai, Y.-W., *J. Appl. Polym. Sci.*, 88(5) 1384-1392, 2003.
21. Xie, X.L., Fung, K.L., Li, R.K.Y., Tjong, S.C. and Mai, Y.-W., *J. Polym. Sci.*, B40(12) 1214-1222, 2002.
22. Tjong, S.C. and Meng, Y.Z., *J. Polym. Sci.*, B41(19) 2332-2341, 2003.
23. TS EN ISO 180: Plastics - Determination of Izod impact strength, 2006.
24. Kinloch, A.J. and Young, R.J., "Fracture Behaviour of Polymers", Elsevier Applied Science Publishers Ltd., London, 1983.
25. Karger-Kocsis, J., "Polypropylene Structure, Blends and Composites", Vol. 3 Composites, Chapman & Hall, Cambridge, 1995.
26. Utracki, L.A., "Two-Phase Polymer Systems", Carl Hanser Verlag, Munich, 1991
27. Kwee, T., Mauritz, K.A. and Beyer, F.L., *Polymer*, 46(11) 3871-3883, 2005.
28. Scott, C., Ishida, H. and Maurer, F.H.J., *J. Mater. Sci.*, 22(11) 3963-3973, 1987.
29. Garton, A., "Infrared Spectroscopy of Polymer Blends, Composites and Surfaces", Carl Hanser Verlag, Munich, New York, 1992.
30. Stuart, B., "Infrared Spectroscopy: Fundamental and Applications", John Wiley and Sons Ltd., Sussex, England, 2004.
31. Gaylord, N. G., "Compatibilization of Hydroxyl-Containing Fillers and Thermoplastic Polymers", *UK Patent*, GB 1 300 640, December 20 1972.
32. Gaylord, N. G.: "Compatibilization of Hydroxyl-Containing Fillers and Thermoplastic Polymers", *US Patent*, US 3 956 230, May 11 1976.